



TECHNICAL ARTICLE

# Wetting and Interfacial Chemistry of New Pb-Free Sn-Zn-Ag-Al-Li (SZAAL) Solder with Cu, Ni, and Al Substrates

Aleksandra Dybel , Paweł Czaja , Janusz Sitek , and Janusz Pstruś

Submitted: 18 November 2022 / Revised: 20 February 2023 / Accepted: 24 March 2023 / Published online: 17 April 2023

This paper presents the results of the Ni substrate wetted with the liquid Sn-Zn eutectic alloy with the addition of Ag, Al, and Li (84.3 at.% Sn, 13.7 at.% Zn, 1 at.% Ag, 0.5 at.% Al, and 0.5 at.% Li-SZAAL). The wetting tests were performed using two methods: the wetting balance tests (WBT) and the sessile drop (SD) method at 250 °C, in the presence of an ALU33® flux. The wetting times were 5, 20, 60, 180, and 1800 s. Next, the microstructure of selected solidified solder joints was investigated using scanning electron microscope. The Ni-Zn system's intermetallic phases (IMCs) were identified at the solder–Ni substrate interface. The kinetics of the formation and growth of the IMC layer was determined. Interfacial tension and contact angle (CA) values were calculated from WBT measurements in the presence of the ALU33® flux. Interfacial tension was compared to surface tension from the maximum bubble pressure and CA values to those obtained using the SD method. The value of the contact angle of SZAAL on Cu (39°) substrate is lower than on Ni (43°). For the comparison, also the interaction between SZAAL and Cu substrate was measured. After 1800 s, the IMCs thickness is significantly reduced for Ni pad than for Cu substrate. The study found that the addition of Al, Ag, and Li improved the tensile strength and wettability of Sn-Zn eutectic-based alloys.

**Keywords** IMC, interfaces, interfacial tension, lead-free solder, Sn-Zn, wetting

## 1. Introduction

The EU RoHS directive (Ref 1) urged the world industry to use lead-free solders. For that process, mainly SACs (Sn-Ag-Cu) and Sn-Zn eutectic-based alloys were used. Solder alloys based on Sn-Zn eutectic are competitive to those commonly employed in electronics, like Sn-Ag and SAC-based alloys with eutectic composition, due to their lower melting point, avoidance of detrimental whiskers in connections, better physico-chemical and mechanical properties, and lower manufacturing costs (Ref 2, 3). Those alloys turned out to be useful in joining aluminum with different materials, especially Cu and Ni (Ref 4). However, the search for the Sn-Pb alloy substitute continues

due to the disadvantages of the currently used materials. That is why those alloys are still being optimized to meet the technological requirements, like providing low melting point, good electrical conductivity and wettability, sufficient mechanical properties, and a favorable price. Thus, one of the methods is to adjust the chemical composition of the solder. The widely used alloying elements are, for instance, Ag, Cu, In, and Bi (Ref 5). Hence, the following alloying additions of the Sn-Zn system were selected: Al, Ag, and Li. The additions were expected to improve the oxidation resistance (Al) (Ref 6), increase tensile strength, and reduce electrical resistivity (Ag, Li) (Ref 4), as well as increase spreading velocity and the wettability (Li) (Ref 7).

Another concern in the soldering process is the creation of intermetallic compounds (IMCs) at the liquid/solid interface. In particular, using copper substrates with currently used lead-free alloys results in obtaining IMCs containing Cu and Sn or Zn atoms. The presence of IMCs is a result of diffusion, which confirms a good solder/pad joint. A small percentage of those compounds can cause improvements in thermal and mechanical properties (Ref 8). On the other hand, the excessive growth of IMCs can cause severe problems with connection cracking. Tu et al. showed that the reliability of the joint was correlated with the thickness of IMCs at the interface (Ref 9). Those phases strongly influence the mechanical properties—they reduce the joints' tensile strength (Ref 10) and worsen the electrical properties (Ref 11). Thus, their microstructure has to be known and precisely controlled to obtain a joint with desired properties. Contrary to the layer observed on copper, a single, relatively flat, and very thin intermediate layer forms at the liquid Sn-Zn/Ni substrate interface. Its composition is similar to the  $\gamma$ -Ni<sub>5</sub>Zn<sub>21</sub> phase.

This article is an invited submission to the *Journal of Materials Engineering and Performance* selected from presentations at the 10th International Conference on High Temperature Capillarity (HTC 2022) held September 12–16, 2022, in Kraków, Poland. It has been expanded from the original presentation. The issue was organized by Prof. Natalia Sobczak of the Polish Academy of Sciences.

Aleksandra Dybel, Paweł Czaja, and Janusz Pstruś, Institute of Metallurgy and Materials Science, Polish Academy of Sciences, Reymonta Street 25, 30-059 Krakow, Poland; Janusz Sitek, The Łukasiewicz Research Network - Tele- and Radio Research Institute, Ratuszowa Street 11, Warsaw 03-450, Poland. Contact e-mail: a.dybel@imim.pl.

The results of the previously reported experiments show that the growth rate of the intermetallic phase layer at the Sn-9Zn-x/Cu interface is much higher than at the Sn-9Zn-x/Ni (Ref 12-14).

Cu substrates are nickel-plated to reduce the harmful effect of IMCs excessive formation (Ref 12, 13, 15). Also, the main goal of modification of Sn-Zn-based alloys is to suppress the growth of IMCs. For that reason, the research shown in this work includes the description of the IMCs growth kinetics for Ni pads. For that purpose, samples were held at 250 °C at different times. The obtained information will allow for setting the implementation potential of this experimental solder.

## 2. Experimental Section

For the experiments, pure Sn (99.999%), Zn (99.95%), Ag (99.999%), Al (99.95%), and Li (99.95%) were used to produce SZAAL (84.3 at.% Sn, 13.7 at.% Zn, 1 at.% Ag, 0.5 at.% Al, and 0.5 at.% Li) solder alloy. The melting procedure followed the one described by Pstruś (Ref 16). The sessile drop (SD) method, described elsewhere (Ref 16), was used for wetting experiments. The procedure previously reported and developed for Cu pads was implemented for Ni substrates, which were covered by a thin flux film and put into a furnace. At the experiment temperature, 0.5 g of SZAAL solder, covered with the ALU33® flux, was introduced into a furnace with a separate dispenser. The flux components are aminoethylethanolamine (C<sub>4</sub>H<sub>12</sub>N<sub>2</sub>O) and ammonium fluoroborate (NH<sub>4</sub>BF<sub>4</sub>). According to ISO 9454-1, this is the 2.1.2-type flux, i.e., organic, water-soluble, and activated with halides. After a few seconds, the molten metal fell onto an investigated substrate, and time was counted accordingly to the experiment. Next, the sample was moved into a cold zone and cooled with room-temperature water. Moreover, measurements of the wettability of the above-mentioned solder were taken on Al (*T* = 250 °C, time: 60 s) and Cu (*T* = 250 °C, time: 1800 s) substrates. IMCs growth kinetics on Ni was determined by performing tests at a constant temperature of 250 °C, for different times: 5 s, 20 s, 1 min, 3 min, and 30 min. For statistical purposes, each variant of the experiment was performed 5 times.

Images of the samples following heat treatment were taken at top and side views. Contact angles and the values of solder spread area were obtained from the image analysis using ImageJ software (Ref 17), followed by calculating the mean values. The solidified samples were cut parallel to the IMCs growth direction and prepared for scanning electron microscopy (SEM) characterization, including resin mounting, polishing, and deposition of a thin carbon film to prevent electric charge accumulation. SEM imaging was carried out on samples' cross sections using FEI E-SEM XL30 microscope in backscattered electron (BSE) mode (20 keV, WD = 10 mm). Chemical analysis was carried out with EDX spectrometer X EDAX GEMINI 4000. The thickness of IMCs was calculated from the SEM images using ImageJ software.

A wetting balance test (Ref 18) (WBT) was applied for SZAAL solder and Ni substrates in the presence of ALU33® flux using the Menisco ST88 device (Metronelec, France). It is a quantitative solderability test introduced by Miyazaki (Ref 19) used to measure the wetting forces between molten solder and the test surface as a function of time. Using this

relationship, the contact angle  $\Theta$  is calculated using the following formula:

$$\cos\Theta = \frac{F_r + \rho \cdot V \cdot g}{\gamma_{LV} \cdot l} \quad (\text{Eq 1})$$

where  $F_r$  is the resultant force of vertical forces of buoyancy and surface tension,  $\gamma_{LV}$  denotes the molten solder–vapor surface tension or solder–flux interfacial tension,  $l$  states for the perimeter of the sample in the meniscus area,  $\rho$  is the density of the solder at the tested temperature,  $V$  refers to the volume of the immersed part of the tested sample, and  $g$  is gravity (9.81 cm/s<sup>2</sup>).

To obtain the values of the contact angle for SZAAL solder and Ni samples in the presence of ALU33® flux, the interfacial tension is needed, according to Eq 1. That is why, tests with non-wetting PFTE rods as tested samples were also performed (in this case  $\cos\Theta = -1$ ), and the value of  $\gamma_{LV}$  for each investigated temperature (250, 275, and 300 °C) was calculated using Eq 2:

$$\gamma_{LV} = \frac{F_r - \rho \cdot g \cdot h \cdot P}{l} \quad (\text{Eq 2})$$

where  $P$  is the area of the immersed part of the PFTE rod,  $h$  denotes the immersion depth, and  $F_r$  is the value of the resultant force, where the force–depth relationship is linear.

The parameters used for the WBT experiments performed in air: Ni substrate immersion speed was 21 mm/s and immersion depth – 5 mm. Substrates were in the solder bath for 10 s. The contact angle was calculated from the force versus time function, using the force value after 3 s of immersion. The wetting time (Table 1) refers to the time elapsed from the moment of contact with the solder surface until the contact angle between the solder and the metallic surface is 90°. For reliable results, five specimens per condition were used.

## 3. Results and Discussion

### 3.1 Wetting Properties

Evaluation of the wettability of the nickel substrate with the SZAAL solder was carried out using two methods, sessile drop method (SD) and wetting balance method (WBT), while that of copper and aluminum substrates were assessed only by the SD method.

**3.1.1 Sessile Drop Method (SD).** The results of the wettability measurements are shown in Fig. 1 and 2, for a spreading area of 0.5 g of SZAAL and contact angles for different substrates, respectively. The given values are the mean of 5 measures.

The observed contact angle values for Cu substrate at 250 °C (39°) are similar to the one described so far in the

**Table 1 Wetting times ( $\tau_z$ ) and maximum forces ( $F_{\max}$ ) for SZAAL/Ni couple using WBT**

Temperature, °C	$\tau_z$ ( $\theta = 90^\circ$ ), s	$F_{\max}$ , mN
250	1.68 ± 0.05	5.15 ± 0.71
275	1.66 ± 0.20	4.82 ± 0.10
300	1.23 ± 0.09	5.79 ± 0.99

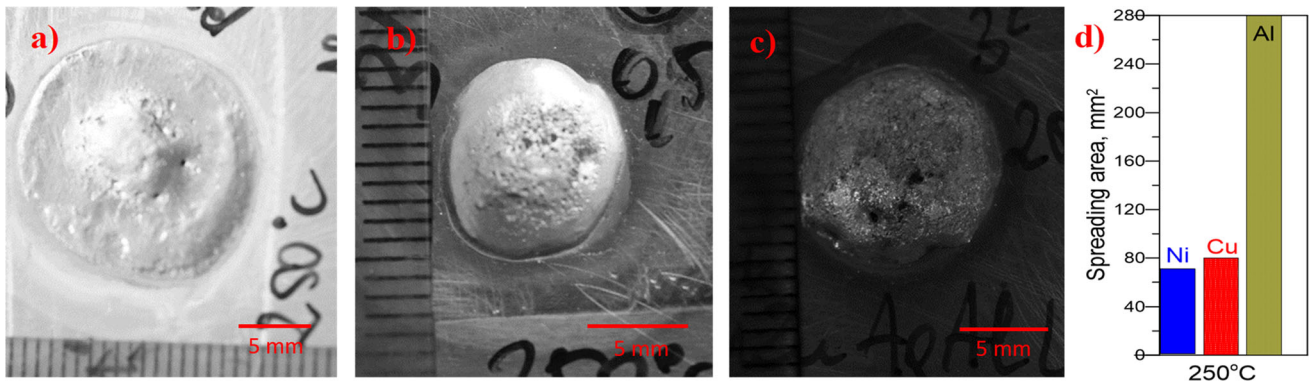


**Fig. 1** Top-view photographs of solidified sessile drop samples (0.5 g) of SnZnAgAlLi solder, after testing at 250 °C, on aluminum (a), copper (b), nickel (c), and measurements of corresponding spreading area (d)

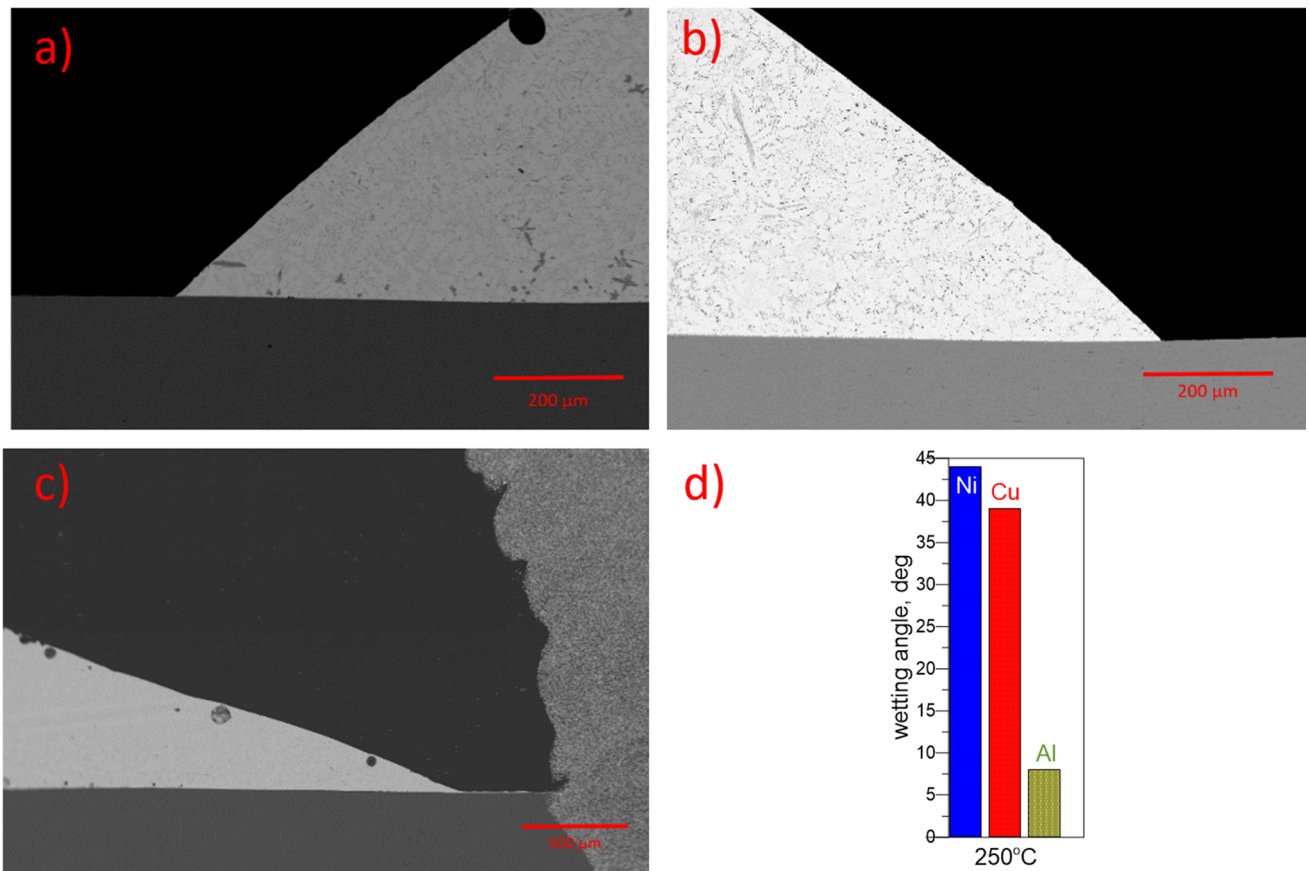


**Fig. 2** SEM images of cross-sectioned sessile drop couples with SnZnAgAlLi (SZAAL) solder, after testing at 250 °C, on different substrates: Ni (a), Cu (b), Al (c), and measurements of corresponding contact angles (d)

literature for Sn-Zn eutectic,  $(\text{SnZn})_{\text{eut}} + \text{Cu}$  (Ref 20-22), as well as  $(\text{SnZn})_{\text{eut}} + \text{In}$  alloys (Ref 14). However, the values of contact angle for SZAAL on Cu substrate are significantly lower than those reported by Cheng et al. (Ref 23). The difference may be a result of using different flux in the mentioned work, which deoxidizing effect on the metallic surface may have been insufficient. For nickel substrates, the contact angle values are in the range between 43° and 46°, which is consistent with previously reported works (Ref 14, 22). The value of the contact angle of SZAAL on Al pads

(8°) is a few times lower than on Ni (43°) and Cu (39°) and relates to values described elsewhere (Ref 20). It is widely accepted in electronic industry that the contact angles below 20° indicate very good, in a range of 30°-40°—good, and those of 40°-50°—sufficient wetting (Ref 24). In the case of Al substrate (Fig. 2c), many pores are visible on the solders' top surface. Probably, due to the relatively high spreading speed of liquid solder on the aluminum surface, flux vapors were trapped in the solder during the wetting process.

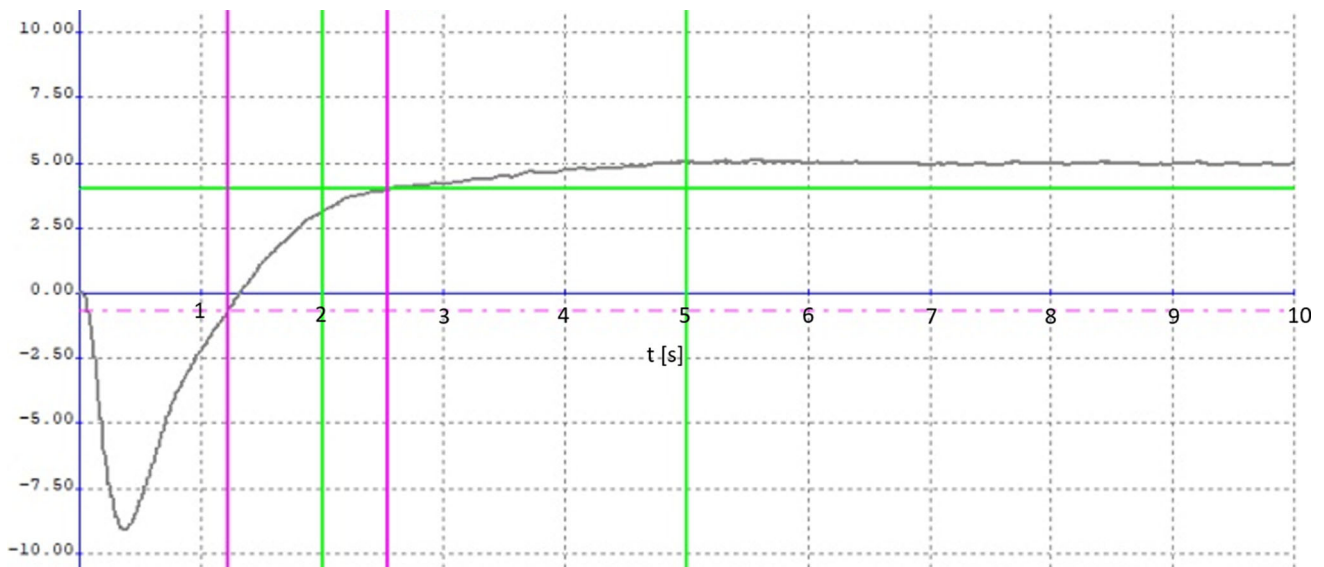


**Fig. 3** Average MBT wetting curve for Ni pad covered with ALU33® flux and wetted by SZAAL at 300 °C in air atmosphere

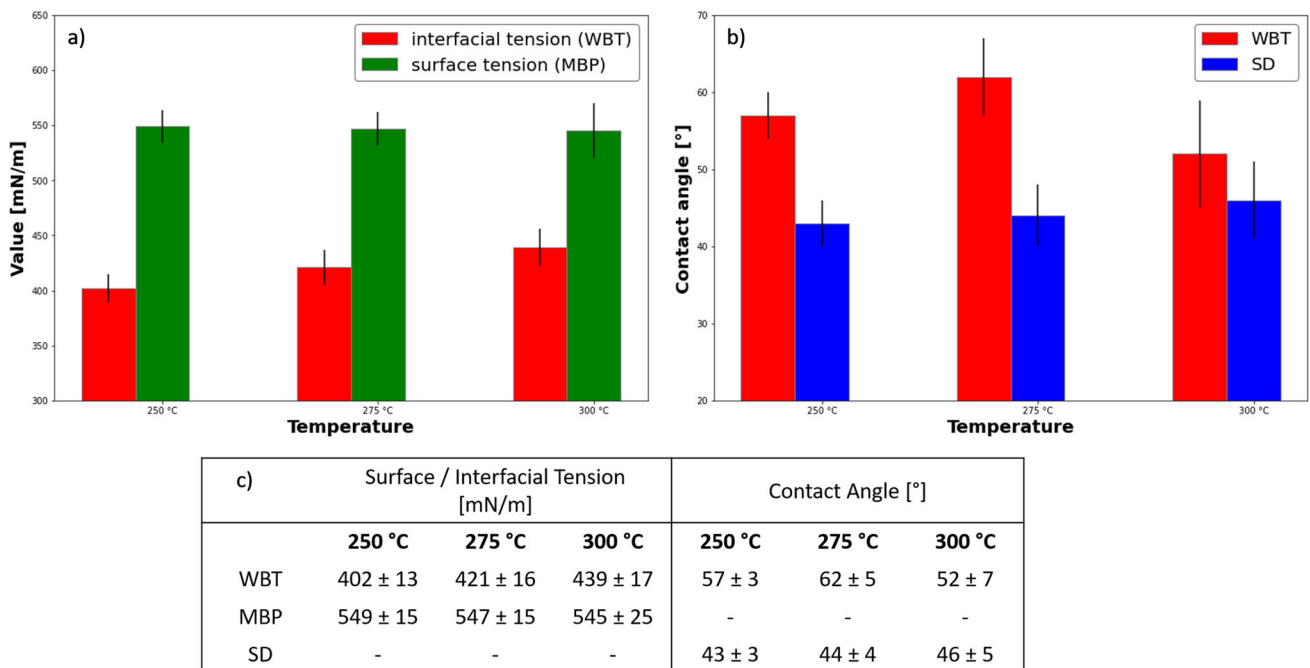


**Fig. 4** Comparison of WBT interfacial tension with surface tension results from maximum bubble pressure (MBP) method (a), and contact angle values for WBT and for SD (b), (a) and (b), with corresponding values (c). Wetting balance method, maximum bubble pressure method, and sessile drop method are marked with red, green, and blue color, respectively

**3.1.2 Wetting Balance Method (WBT).** Wetting tests of Ni substrates using the WBT method were performed at temperatures of 250, 275, and 300 °C, in the presence of ALU33® flux in the air atmosphere. The test results are shown in Table 1 and Fig. 3 and 4.

The interfacial tension determined by the WBT is much lower than the surface tension obtained by the maximum bubble pressure (MBP) method (Fig. 4a). It is related to the use of the flux in the WBT method which reduces the interfacial tension. Additionally, an increase in the interfacial tension and a decrease in the surface tension with temperature are observed.

Based on the average wetting curve (Fig. 3) obtained from the WBT experiment, the contact angle (Fig. 4b), wetting

maximum force, and wetting time are determined (Table 1). The lower contact angle obtained by the SD method, compared to WBT, is related to the use of a protective atmosphere in this method. Wetting time decreases with increasing temperature, while in the case of wetting maximum force there is no clear dependence; at temperature of 300 °C, the force is the highest, but at  $T = 275$  °C it is lower than for  $T = 250$  °C.

### 3.2 SEM Observations

As a result of the reaction of the liquid solder with the Ni substrate, grains of the intermetallic phase were formed at the interface (Fig. 5 and 6). The EDS results demonstrate that the

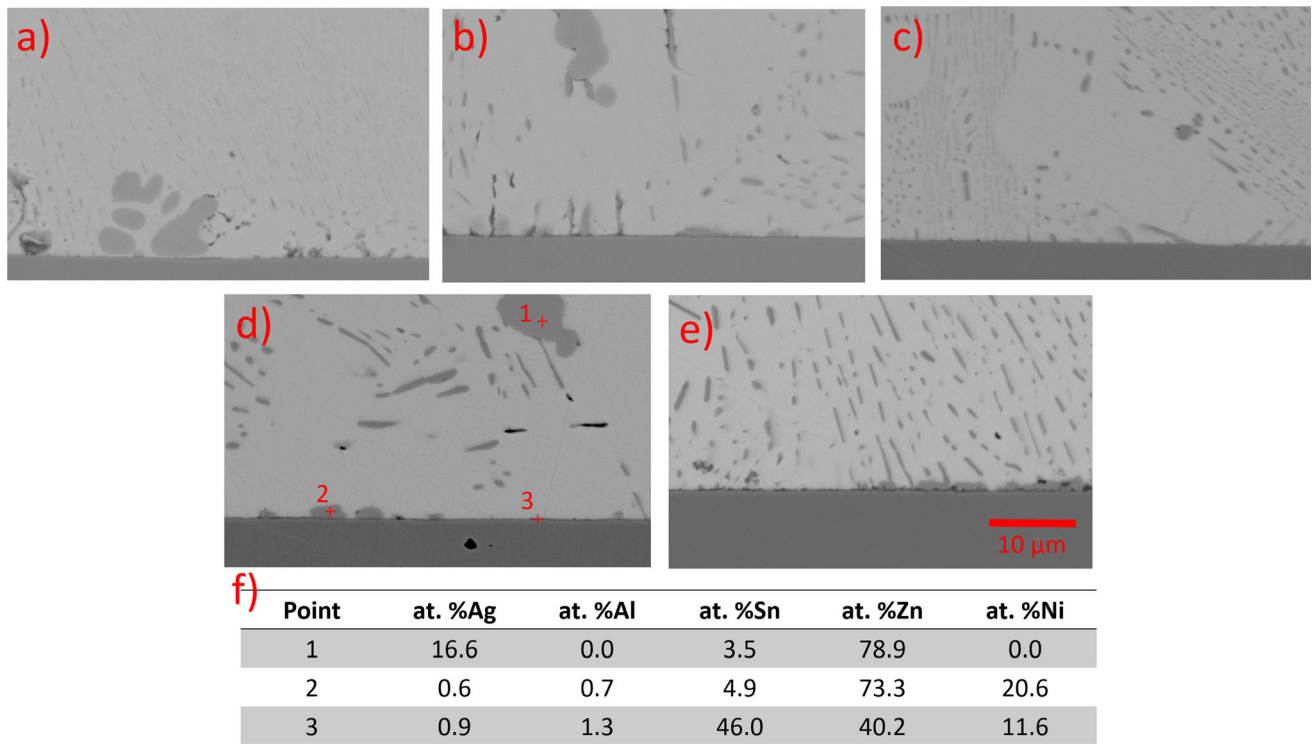


**Fig. 5** SEM micrographs of SZAAL/Ni interface at the test temperature after different contact times: (a) 5 s, (b) 20 s, (c) 60 s, (d) 180 s, and (e) 1800 s with table with EDS results (f) for corresponding points marked above. The scale bar refers to all of the images

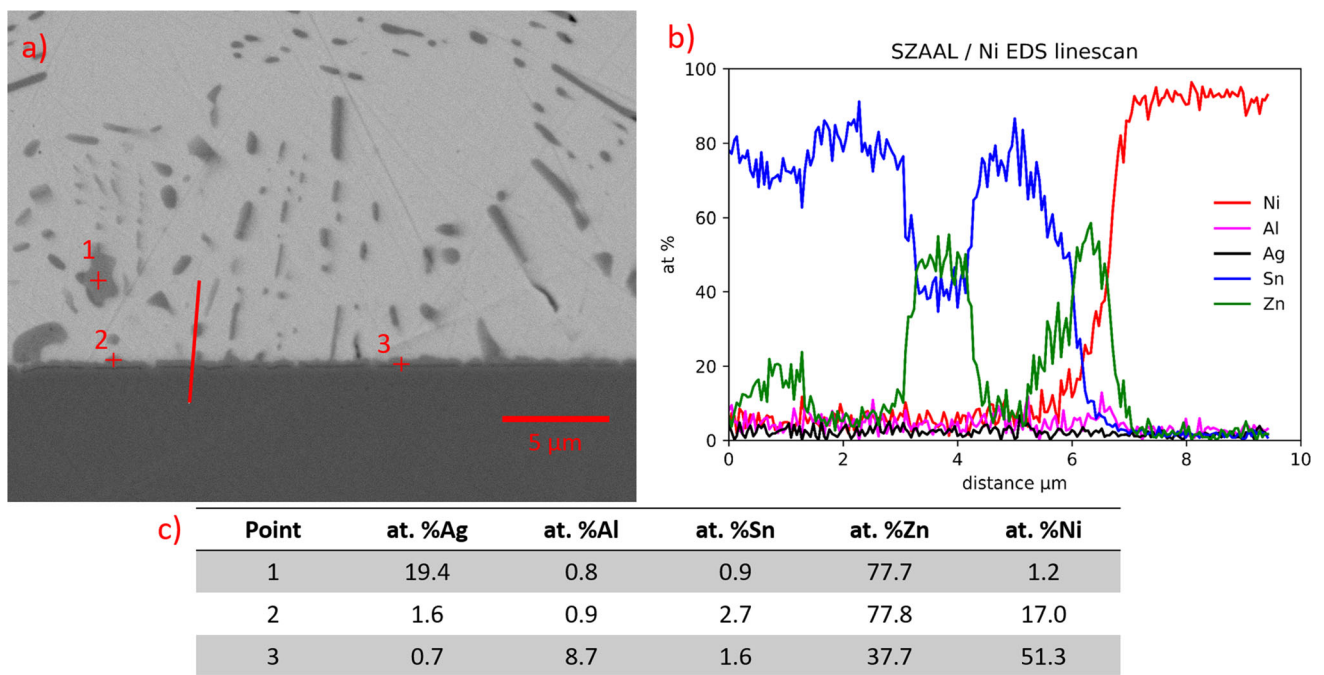


**Fig. 6** SEM micrograph SZAAL/Ni interface after 1800 s of contact (a) with EDX line scan (b) and point analysis results (c)

$\text{Ni}_5\text{Zn}_{21}$  phase is present. The EDS results are given for clarity in tables—Fig. 5(f) and 6(c). The grains of this phase grow with the wetting time and a continuous layer of the phase was observed after 1800 s of heating at 250 °C (Fig. 6). Here, it has

to be emphasized that the layer is most likely formed in the time interval between 180 and 1800 s, and since the microstructural analysis is performed after 1800 s, it is difficult to determine the exact time when the layer becomes continuous. Wang et al.

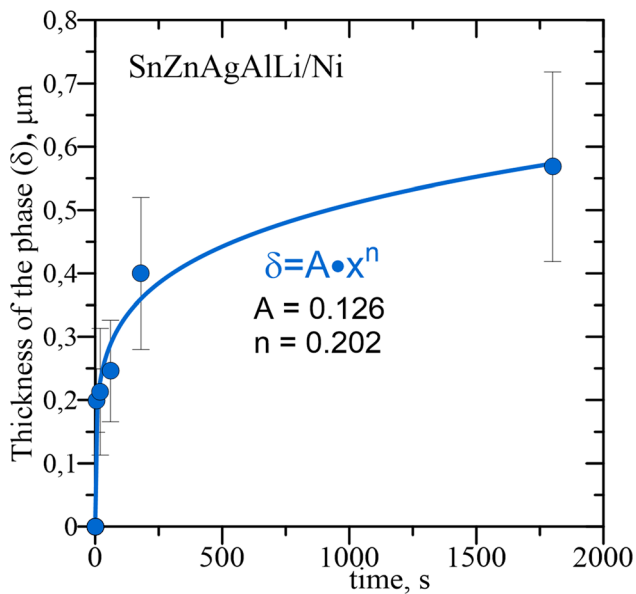


Fig. 7 IMC thickness as a function of contact time with the fitted curve

obtained similar results (Ref 25), where they noticed a uniform  $\text{Ni}_5\text{Zn}_{21}$  layer that grew continuously with the reaction time for Zn content higher than 5 wt.%.

Moreover, SEM images also showed spheroidal precipitates. The EDS analysis confirmed that they are composed mainly of Zn and Ag, corresponding to  $\text{AgZn}_3$  intermetallic (Ref 25, 26). Linescan and point EDS analysis did not show the presence of Ag in the matrix nor at the interface. Taking into consideration the above, the following conclusion could be made that all of the silver was consumed to create  $\text{AgZn}_3$  precipitates. This phase enhanced the tensile strength of the joints.

Using SEM images of SZAAL/Ni interfaces formed after different holding times at the test temperature, the thickness of the IMC layer was determined. Then, a plot of thickness versus time was created. For the given data points, the fitting procedure was applied and the equation of the curve was found to be  $y = 0,126x^{0,202}$  (Fig. 7). It is worth mentioning that the thickness of the IMC for SZAAL wetting Ni pad is significantly lower than other Sn-Zn eutectic-based alloys. In the present work, after 60 s, the thickness was  $0.25 \mu\text{m}$ , and after 1800 s, it was  $0.55 \mu\text{m}$ . In other reports, for Sn-Zn<sub>eut</sub>  $1 \mu\text{m}$  was obtained after 30 s (Ref 27), and for 900 s,  $5\text{-}\mu\text{m}$ -thick IMC was observed (Ref 14). Such a massive drop in IMC thickness may be a result of Al and Li atoms in the interfacial area. The EDX line scan shown in Fig. 5 shows that Al atoms are solved in the gamma phase, substituting Zn ( $\gamma\text{-Ni}_5\text{Zn}(\text{Al})_{21}$ ) and grouped at the interface in the vicinity of the Ni pad. Thus, it could be deduced that Al hinders the interfacial diffusion process, contributing to the reduction in the thickness of the IMC layer. It can be assumed that lithium acts differently than Al. The wetting tests were performed with the flux but without a protective atmosphere. Therefore, lithium could easily form oxides and nitrides since it is a very active element. Li atoms

are absorbed in the active sites on the Ni surface (Ref 16) and form  $\text{Li}_3\text{N}$  nitride, blocking the diffusion of Ni substrate atoms to the solder and Zn atoms from the liquid alloy toward the substrate. However, the  $\text{Li}_3\text{N}$  layer is not continuous; thus, IMCs form at places where the Ni substrate is exposed to the solder. With the annealing time, IMCs grow and create characteristic scallops (Fig. 5). Parallel to those processes, the surface diffusion of Zn atoms on the Ni pad occurs even under the lithium nitride layer. The continuous IMC layer is formed (Fig. 6) between 3 and 30 min of annealing. However, the explanation of this phenomenon needs further research.

For the comparison, also the interaction between SZAAL and Cu pad is shown in Fig. 8. After 1800 s, the IMCs thickness is significantly reduced for Ni pad than for Cu substrate. In the case of Cu substrate, three layers of IMCs were observed: From the Cu side, there is a thin layer of  $\beta\text{-CuZn}$  phase, next there is area identified as  $\gamma\text{-Cu}_5\text{Zn}_8$ , and also, there is  $\varepsilon\text{-CuZn}_4$  phase from the solder side. Similar observations were made by Pstruś et al. (Ref 28). The results justifies the process of nickel plating of copper pads to obtain more favorable, thinner layer of intermetallics at the solid-liquid interface.

Also other type of interaction of solid substrate-liquid SZAAL solder is possible. The mechanism of pad dissolution is shown in the case of Al substrate in Fig. 9. Here, the formation of IMCs is not observed.

## 4. Conclusions

The interaction of (SnZn)<sub>eut</sub> + 1%Ag + 1%Al + 0.5%Li (at%)—SZAAL alloy with Ni pads is presented in this work. Also, for the comparison, the examples of wetting on Cu and Al substrates were included. The liquid SZAAL solder, while interacting with Cu and Ni substrates, creates an intermediate layer at the interface, containing mostly gamma phases ( $\text{Cu}_5\text{Zn}_8$  and  $\text{Ni}_5\text{Zn}_{21}$ , respectively). IMCs grew much faster on the Cu pad than on Ni. Those compounds decrease the solder properties, especially important in microelectronics, like electrical conductivity and mechanical properties. Therefore, the recommended use of investigated solder is with previously prepared Cu pads, with the Ni layer deposited onto the joining side. Al and Li alloying additives drastically reduced the thickness of the intermetallic layer. However, their influence on the growth kinetics of IMCs requires full explanation and further research. For the Al substrate, the other type of interaction was observed with the dissolution of the pad and IMCs were not detected.

Results from the wetting balance method were compared with the maximum bubble pressure method and sessile drop to determine surface/interfacial tension and contact angles, respectively. The use of ALU33® flux caused a decrease in the values of interfacial tension. Higher values of contact angles for WBT than SD were induced by using a protective atmosphere in the case of SD.

The addition of Al, Ag, and Li to Sn-Zn eutectic-based alloys can improve their oxidation resistance, tensile strength,

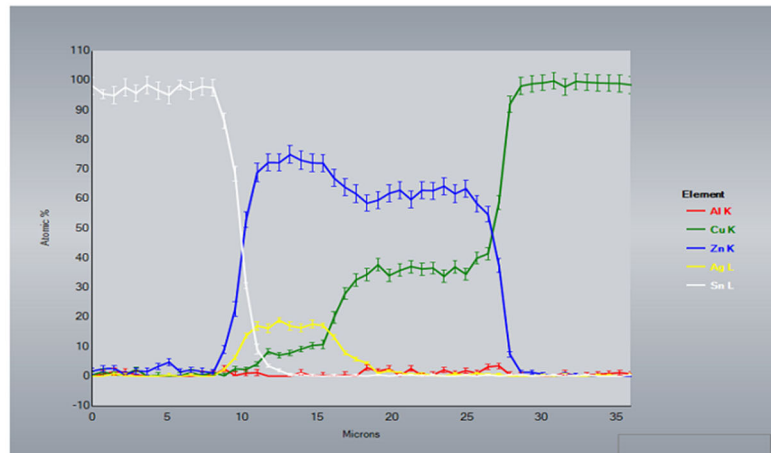
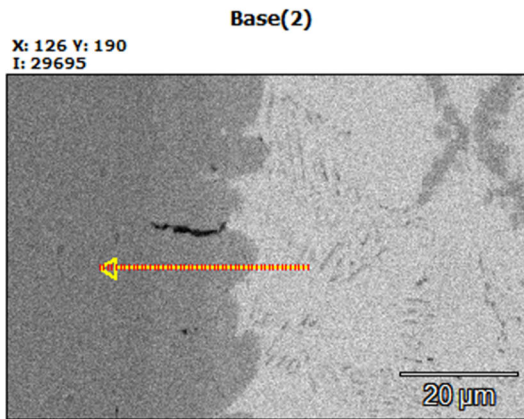
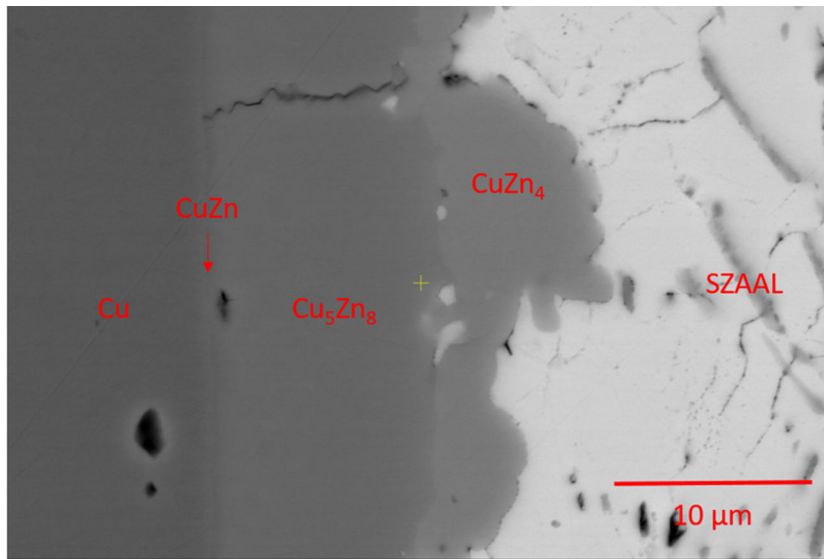


**Fig. 8** SEM image of SZAAL-Cu interface after 1800 s of contact at 250 °C (a), SEM image showing the line chosen for EDS analysis (b), results of the EDX line scan investigation (c)

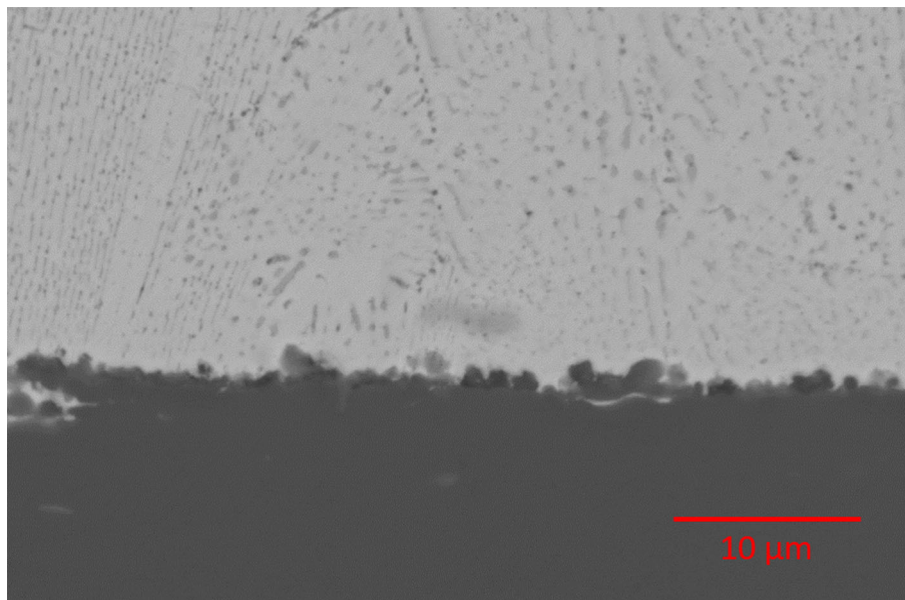


**Fig. 9** SEM image of SZAAL-Al interface after 60 s contact at 250 °C

and wettability. This study's results could contribute to the development of optimized Sn-Zn eutectic-based alloys for joining aluminum with other materials.

## Acknowledgments

The authors acknowledge the financial support from the National Science Centre Poland, Project No 2018/29/B/ST8/02558.

## Open Access

This article is licensed under a Creative Commons Attribution 4.0 International License, which permits use, sharing, adaptation, distribution and reproduction in any medium or format, as long as you give appropriate credit to the original author(s) and the source, provide a link to the Creative Commons licence, and indicate if changes were made. The images or other third party material in this article are included in the article's Creative Commons licence, unless indicated otherwise in a credit line to the material. If material is not included in the article's Creative Commons licence and your intended use is not permitted by statutory regulation or exceeds the permitted use, you will need to obtain permission directly from the copyright holder. To view a copy of this licence, visit <http://creativecommons.org/licenses/by/4.0/>.

## References

1. E. Parliament and C. of the E. Union, Directive 2011/83/EU of the European Parliament and of the Council, *Fundam. Texts Eur. Priv. Law*, 2020, p 88–110
2. S. Vaynman, G. Ghosh, and M.E. Fine, Some Fundamental Issues in the Use of Zn-Containing Lead-Free Solders for Electronic Packaging, *Mater. Trans.*, 2004, **45**(3), p 630–636
3. J. Villain, W. Jilck, E. Schmitt, and T. Qasim, No Title, *Proc. 2004 Int. IEEE Conf. Asian Green Electron. AGECE (IEEE Cat. No. 04EX769)*, 2004, p 38–41
4. M.L. Huang, Y.Z. Huang, H.T. Ma, and J. Zhao, Mechanical Properties and Electrochemical Corrosion Behavior of Al/Sn-9Zn-XAg/Cu Joints, *J. Electron. Mater.*, 2011, **40**(3), p 315–323
5. T. Laurila, V. Vuorinen, and M. Paulasto-Kröckel, Impurity and Alloying Effects on Interfacial Reaction Layers in Pb-Free Soldering, *Mater. Sci. Eng. R Reports*, 2010, **68**(1–2), p 1–38
6. K.L. Lin, L.H. Wen, and T.P. Liu, The Microstructures of the Sn-Zn-Al Solder Alloys, *J. Electron. Mater.*, 1998, **27**(3), p 97–105
7. Z. Moser, W. Gąsior, J. Pstruś, K. Kujawa-Bukat, J. Sitek, and J. Kościelski, Lead-Free, Modified Tin-and-Zinc Solder for Soft Soldering, Poland, 2014
8. P.G. Harris and K.S. Chaggar, The Role of Intermetallic Compounds in Lead-Free Soldering, *Solder. Surf. Mt. Technol.*, 1998, **10**(3), p 38–52
9. P.L. Tu, Y.C. Chan, and J.K.L. Lai, Effect of Intermetallic Compounds on the Thermal Fatigue of Surface Mount Solder Joints, *IEEE Trans. Compon. Packag. Manuf. Technol. Part B*, 1997, **20**(1), p 87–93
10. X. Ma, Y. Qian, and F. Yoshida, Effect of La on the Cu-Sn Intermetallic Compound (IMC) Growth and Solder Joint Reliability, *J. Alloys Compd.*, 2002, **334**(1–2), p 224–227
11. Y. Yao, J. Fry, M.E. Fine, and L.M. Keer, The Wiedemann-Franz-Lorenz Relation for Lead-Free Solder and Intermetallic Materials, *Acta Mater.*, 2013, **61**(5), p 1525–1536
12. Y.C. Chan, M.Y. Chiu, and T.H. Chuang, Intermetallic Compounds Formed during the Soldering Reactions of Eutectic Sn-9Zn with Cu and Ni Substrates, *Int. J. Mater. Res.*, 2002, **93**(2), p 95–98
13. C. Chou, S. Chen, and Y. Chang, Interfacial Reactions in the Sn-9Zn-(x Cu)/Cu and Sn-9Zn-(x Cu)/Ni Couples, *J. Mater. Res.*, 2006, **21**(7), p 1849–1856
14. P. Fima, T. Gancarz, J. Pstruś, and A. Sypień, Wetting of Sn-Zn-XIn (x = 0.5, 1.0, 1.5 wt.%) Alloys on Cu and Ni Substrates, *J. Mater. Eng. Perform.*, 2012, **21**(5), p 595–598
15. J. Peng, R.C. Wang, M. Wang, and H.S. Liu, Interfacial Microstructure Evolution and Shear Behavior of Au-Sn/Ni-XCu Joints at 350 °C, *J. Electron. Mater.*, 2017, **46**(4), p 2021–2029
16. J. Pstruś, Early Stages of Wetting of Copper by Sn-Zn Eutectic Alloy, *J. Mater. Sci. Mater. Electron.*, 2018, **29**(24), p 20531–20545
17. M.D. Abramoff, P.J. Magalhães, and S.J. Ram, Image Processing with ImageJ, *Biophotonics Int.*, 2004, **11**(7), p 36–41
18. Z. Moser, P. Fima, K. Bukat, J. Sitek, J. Pstruś, W. Gąsior, M. Kościelski, and T. Gancarz, Investigation of the Effect of Indium Addition on Wettability of Sn-Ag-Cu Solders, *Solder. Surf. Mt. Technol.*, 2011, **23**, p 22–29
19. M. Miyazaki, M. Mizutani, T. Takemoto, and A. Matsunawa, Conditions for the Measurement of Surface Tension of Solders with a Wetting Balance Tester (Materials, Metallurgy & Weldability), *Trans. JWRI*, 1997, **26**(1), p 81–84
20. P. Fima, J. Pstruś, and T. Gancarz, Wetting and Interfacial Chemistry of SnZnCu Alloys with Cu and Al Substrates, *J. Mater. Eng. Perform.*, 2014, **23**(5), p 1530–1535
21. Y.C. Chan, M.Y. Chiu, and T.H. Chuang, Intermetallic Compounds Formed During the Soldering Reactions of Eutectic Sn-9Zn with Cu and Ni Substrates, *Z. Met.*, 2002, **93**(2), p 95–98
22. C.W. Huang and K.L. Lin, Wetting Properties of and Interfacial Reactions in Lead-Free Sn-Zn Based Solders on Cu and Cu Plated with an Electroless Ni-P/Au Layer, *Mater. Trans.*, 2004, **45**(2), p 588–594
23. S.C. Cheng and K.L. Lin, The Thermal Property of Lead-Free Sn-8.55Zn-1Ag-XAl Solder Alloys and Their Wetting Interaction with Cu, *J. Electron. Mater.*, 2002, **31**(9), p 940–945
24. R.J. Klein-Wassink, Soldering in Electronics 2nd Edition (Isle of Man.), Electrochemical Publications LTD, 1989
25. M.L. Huang, X.L. Hou, N. Kang, and Y.C. Yang, Microstructure and Interfacial Reaction of Sn-Zn-x(Al, Ag) near-Eutectic Solders on Al and Cu Substrates, *J. Mater. Sci. Mater. Electron.*, 2014, **25**(5), p 2311–2319
26. J.E. Lee, K.S. Kim, M. Inoue, J. Jiang, and K. Sugauma, Effects of Ag and Cu Addition on Microstructural Properties and Oxidation Resistance of Sn-Zn Eutectic Alloy, *J. Alloys Compd.*, 2008, **454**(1–2), p 310–320
27. C.H. Wang and H.H. Chen, Study of the Effects of Zn Content on the Interfacial Reactions between Sn-Zn Solders and Ni Substrates at 250 °C, *J. Electron. Mater.*, 2010, **39**(11), p 2375–2381
28. J. Pstruś, P. Fima, and T. Gancarz, Wetting of Cu and Al by Sn-Zn and Zn-Al Eutectic Alloys, *J. Mater. Eng. Perform.*, 2012, **21**(5), p 606–613

**Publisher's Note** Springer Nature remains neutral with regard to jurisdictional claims in published maps and institutional affiliations.